Observations of the spatial and temporal structure of field-aligned beam and gyrating ring distributions at the quasi-perpendicular bow shock with Cluster CIS

E. Möbius, H. Kucharek, C. Mouikis, E. Georgescu, L. M. Kistler, M. A. Popecki, M. Scholer, J. M. Bosqued, H. Rème, C. W. Carlson, et al.

Annales Geophysicae (2001) 19: 1411–1420 © European Geophysical Society 2001

Annales Geophysicae

Observations of the spatial and temporal structure of field-aligned beam and gyrating ring distributions at the quasi-perpendicular bow shock with Cluster CIS

E. Möbius[1], H. Kucharek[2], C. Mouikis[1], E. Georgescu[2], L. M. Kistler[1], M. A. Popecki[1], M. Scholer[2], J. M. Bosqued[3], H. Rème[3], C. W. Carlson[5], B. Klecker[2], A. Korth[6], G. K. Parks[5], J. C. Sauvaud[3], H. Balsiger[4], M.-B. Bavassano-Cattaneo[8], I. Dandouras[3], A. M. DiLellis[8], L. Eliasson[9], V. Formisano[8], T. Horbury[10], W. Lennartsson[7], R. Lundin[9], M. McCarthy[11], J. P. McFadden[5], and G. Paschmann[2]

[1]Dept. of Physics and Institute for the Study of Earth, Oceans and Space, University of New Hampshire, Durham, NH, USA
[2]Max-Planck-Institut für extraterrestrische Physik, Garching, Germany
[3]Centre d'Etude Spatiale et Rayonnement, Toulouse, France
[4]Physikalisches Institut der Universität Bern, Switzerland
[5]Space Sciences Laboratory, University of California, Berkeley, USA
[6]Max-Planck-Institut für Aeronomie, Katlenburg-Lindau, Germany
[7]Lockheed-Martin Palo Alto Research Laboratory, Palo Alto, USA
[8]Istituto di Fisica dello Spazio Interplanetario, Rome, Italy
[9]Institut for Rømdfysik, Kiruna, Sweden
[10]Imperial College, London, UK
[11]Space Program, University of Washington, USA

Received: 16 April 2001 – Revised: 29 July 2001 – Accepted: 4 September 2001

Abstract. During the early orbit phase, the Cluster spacecraft have repeatedly crossed the perpendicular Earth's bow shock and provided the first multi-spacecraft measurements. We have analyzed data from the Cluster Ion Spectrometry experiment (CIS), which observes the 3D-ion distribution function of the major species in the energy range of 5 eV to 40 keV with a 4 s resolution. Beams of reflected ions were observed simultaneously at all spacecraft locations and could be tracked from upstream to the shock itself. They were found to originate from the same distribution of ions that constitutes the reflected gyrating ions, which form a ring distribution in the velocity space immediately upstream and downstream of the shock. This observation suggests a common origin of ring and beam populations at quasi-perpendicular shocks in the form of specular reflection and immediate pitch angle scattering. Generally, the spatial evolution across the shock is very similar on all spacecraft, but phased in time according to their relative location. However, a distinct temporal structure of the ion fluxes in the field-aligned beam is observed that varies simultaneously on all spacecraft. This is likely to reflect the variations in the reflection and scattering efficiencies.

Key words. Interplanetary physics (planetary bow shocks; energetic particles; instruments and techniques)

Correspondence to: E. Möbius
(eberhard.moebius@unh.edu)

1 Introduction

Early observations of energetic ions upstream of the Earth's bow shock were reported by Asbridge et al. (1968), Lin et al. (1974) and West and Buck (1976). These observations demonstrated clearly that the Earth's bow shock is a formidable particle accelerator at our front door step. With its accessibility to a fleet of increasingly sophisticated spacecraft, it presents an excellent natural laboratory for the study of collisionless shocks and is a model for even more powerful, but much more remote, shock waves in a variety of astrophysical settings. Due to the natural variations in the solar wind and the interplanetary magnetic field (IMF), and in the topology of the Earth's bow shock, a wide dynamic range of the controlling parameters and different shock orientations can be studied during repetitive crossings of the Earth orbiting spacecraft. According to the angle Θ_{BN} between the IMF and the shock normal, shocks are usually separated into two distinct parameter regimes, the quasi-perpendicular shock for $\Theta_{BN} > 45°$ and the quasi-parallel shock for $\Theta_{BN} < 45°$. Associated with these two different geometries observations are two distinct and almost mutually exclusive particle populations (e.g. Gosling et al., 1978), which

are referred to as reflected and diffuse components. The reflected ions form a beam directed along the interplanetary magnetic field; these ions are accelerated in a single reflection off the quasi-perpendicular bow shock (e.g. Paschmann et al., 1980) with their energies rarely exceeding $\approx$ 10 keV. They are more commonly called field-aligned beams to distinguish themselves from those reflected ions that are convected downstream as gyrating ions with the IMF. In contrast, diffuse ions upstream of the quasi-parallel shock form a much more isotropic distribution whose energy spectra extend to $\approx$ 200 keV/e (e.g. Scholer et al., 1979; Ipavich et al., 1981). Conversely, the shock structure itself is quite different in these two cases. A sharp and stable transition is usually observed at the quasi-perpendicular shock with a distinct step in the magnetic field and often an overshoot, whereas the quasi-parallel shock appears not as steep and is quite variable in space and time.

In the seventies and early eighties, the Earth's bow shock was primarily described with the tools of an ideal MHD. Particle acceleration was seen as diffusive acceleration due to the compression of the upstream and downstream fluids at the shock (e.g. Axford et al., 1977). A description of the microscopic processes was not available. With a few exceptions, the observations came from a single satellite and required substantial spatial and time averaging. Over the past decade, the advent of hybrid simulations of the shock and the associated ion distributions has led to a revolution in our understanding of the related micro-physics (e.g. Quest, 1988; Burgess, 1989; Scholer and Terasawa, 1990). It was finally realized that the formation of the energetic particle populations that escape into the upstream environment is intimately linked to the very dissipation processes that are at the heart of the shock formation itself. With the launch of the four Cluster satellites, simultaneous observations of fields and particles at four different locations with high time resolution have become available, including the separation of the key species. In addition, the ACE and SOHO spacecraft provide the undisturbed boundary conditions upstream of the shock. Finally, this unique constellation provides a set of tools, with which the shock processes can be studied in the same depth as the detailed modeling is carried out. Anticipated observations and the importance of both the multi-spacecraft observations on varying scales and improved instrumentation have been outlined by Möbius (1995). The synergism between significantly improved modeling and new experimental techniques will allow a much deeper understanding of the cosmic particle accelerator at our front door step.

During the early orbit phase, Cluster primarily encountered a quasi-perpendicular bow shock on the dusk side of the magnetosphere. Therefore, we will limit our preliminary analysis of bow shock related particle distributions to this shock geometry. At the quasi-perpendicular shock, it was recognized earlier than for the parallel shock how intimately ion reflection and acceleration is connected with the dissipation of energy at the shock (Paschmann and Sckopke, 1983). At a quasi-perpendicular shock, the compressed interplanetary magnetic field forms a barrier for the incoming solar wind particles. As a consequence of the different gyroradii of electrons and protons, a repelling electric potential is built up for the protons in the shock layer. A small percentage of the protons is specularly reflected; they gain energy in the convection electric field of the solar wind and then start to gyrate partly upstream and partly downstream of the shock (Sckopke et al., 1990). Immediately downstream of the shock, a ring distribution is observed in addition to the slowed solar wind. Further downstream, after isotropization and thermalization, the ring merges with the bulk flow. The gyration, thermalization and isotropization of the incoming ions is essential to the formation of the hot magnetosheath flow since it provides the mechanism for the conversion of directed energy into heat. However, in the past, this gyrating ring distribution, which extends to about one gyro radius into the upstream region, has been carefully distinguished from the field-aligned beam distribution (e.g. Formisano, 1985; Gosling and Robson, 1985; Thomsen, 1985). While the specular reflection of the gyrating ring distribution has been explained in a straightforward manner as a reflection in the shock potential, the generation of the beam was not so readily understood. Although kinematics and the energetics of the beams is derived correctly in terms of a reflection along the upstream IMF in the deHofman-Teller frame (Sonnerup, 1969; Paschmann et al., 1980), the microphysics of their generation at the shock has been under debate. As an alternative to reflection leakage from the heated magnetosheath distribution has been suggested as the origin of the beams (e.g. Eichler, 1979). Observed distributions that are consistent with this picture, at least for low energy beams, have been observed by Thomsen et al. (1983). However, no general closure on the problem of how to generate the high speed necessary for the ions to escape along the field lines, in particular at shocks with Θ_{BN} close to 90°, has been made. Yet the known effectiveness of quasi-perpendicular shocks to accelerate particles has triggered further theoretical work on what is referred to as the injection problem at quasi-perpendicular shocks. On the one hand, the work has concentrated on shock surfing to achieve the initial energy, but without redistribution, the resulting ion population is swept downstream (e.g. Lee et al., 1996). On the other hand, the possibility of cross-field diffusion at the shock has been considered in order to provide an avenue for escape (e.g. Giacalone et al., 1994; Scholer et al., 2000).

In this paper, we will make use of the capabilities of the CIS instrument on Cluster to gather the 3D distribution function of ions within one spin period (4 s) with good counting statistics. We will follow the reflected ion populations, both field-aligned beam and gyrating ions, from the upstream region into the quasi-perpendicular shock. In addition, we use multi-spacecraft observations of ions and the magnetic field to unambiguously distinguish intrinsic temporal fluctuations in the ion beam intensity from the effects of the relative motion with respect to the shock. It is demonstrated that both beam and gyrating ions apparently emerge from the same process at the shock, whose effectiveness shows significant temporal variations on the scale of less than one minute.

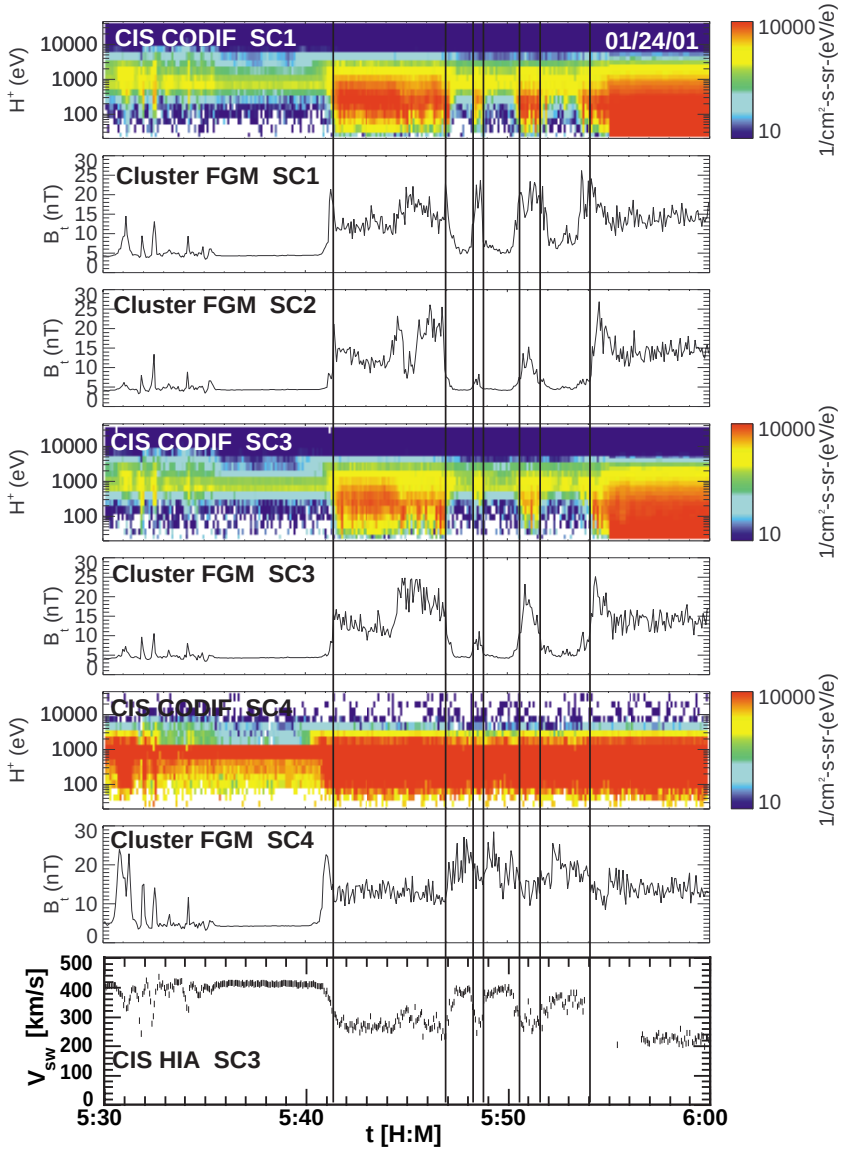

Fig. 1. From top to bottom: colored spectrogram of the H^+ differential particle flux and the magnetic field magnitude $\boldsymbol{B}$ from spacecraft 1, $\boldsymbol{B}$ from spacecraft 2, H^+ and $\boldsymbol{B}$ from spacecraft 3 and spacecraft 4, followed by the H^+ bulk speed from spacecraft 3 for the time period of 05:30–06:00 UT on 24 January 2001. The vertical lines indicate the bow shock crossings of spacecraft 3.

These results may hold the key to the injection problem at quasi-perpendicular shocks, given the opportunity that Cluster will provide such comprehensive observations under a variety of bow shock conditions.

2 Instrumentation and overview of observations

The Cluster Ion Spectrometry (CIS) instrument consists of two complementary sensors. The Composition and Distribution Function (CODIF) analyzer provides the 3D velocity distribution function of the major ion species (H^+, He^{2+}, He^+ and O^+) in the energy range from spacecraft potential to 40 keV/e with a time resolution of up to one spin period. The Hot Ion Analyzer (HIA) provides the 3D velocity distribution with high energy and angle resolution, but without species discrimination. Both sensors are based on a top hat electrostatic analyzer design, which provides a 360° instantaneous field-of-view, which is divided into angular pixels. The other direction is covered by making use of the spacecraft spin through a sectoring scheme. The energy range is covered by logarithmically stepping the analyzer voltage during each sector interval. To provide the necessary dynamic range, the entrance aperture of CODIF is divided into two halves, with a difference in the geometric factor of approximately two orders of magnitude. The mass per charge of each ion is determined by combining the E/Q measurement from the electrostatic analyzer with the post-acceleration of the ions by up to 20 kV and with a time-of-flight measurement. A detailed description of the instruments may be found in Rème et al. (1997) and Möbius et al. (1998). The CIS instruments are operational on spacecraft 1, 3 and 4. On spacecraft 2 CIS is disabled due to an apparent failure of its low voltage power converter. An overview of the instrument capabilities and first observations is given in Rème et al. (2001).

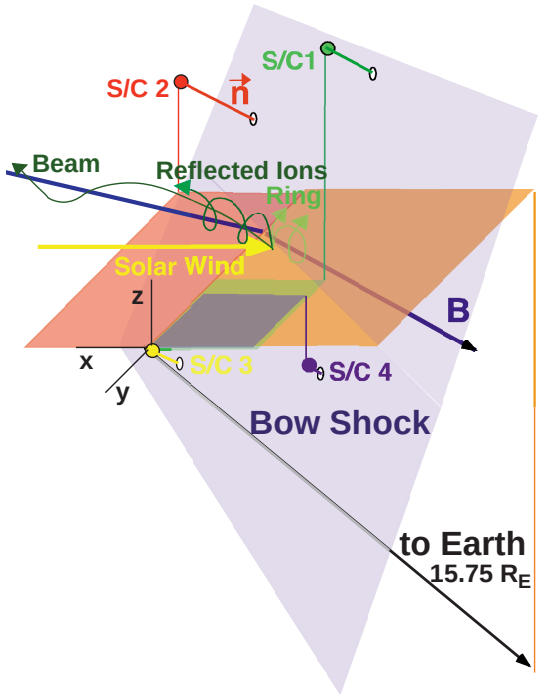

Fig. 2. Orientation of the bow shock at the location of the Cluster spacecraft and their relative position in space for 24 January 2001. The colored areas and the vertical lines indicate the position of spacecraft 1, 2 and 4 relative to the reference spacecraft 3. The spatial orien-tation of the vector pointing towards the Earth is shown in a similar way (not to scale). The short lines from the spacecraft towards the shock (light blue shaded area) indicate the relative distance of the three spacecraft from the shock upon their approach.

The magnetic field information is obtained from the Cluster Flux Gate Magnetometers (FGM) (Balogh et al., 1997).

For our analysis of the bow shock, we have chosen one time period during the early operations phase of Cluster in January 2001 with primarily quasi-perpendicular conditions. On 24 January, the Cluster spacecraft remained almost exactly at the bow shock for an extended period of time with several consecutive crossings of the spacecraft. During this early orbit phase, Cluster was configured as a regular tetrahedron with a nominal separation of about 600 km between neighboring spacecraft. Burst mode telemetry was available during the chosen time interval, and the particle distributions could be obtained with the highest resolution of one spin period.

Figure 1 shows an overview of the temporal evolution as the Cluster spacecraft repeatedly encounter the bow shock during the time interval under investigation (from 05:30 to 06:00 UT on 24 January). Shown are colored spectrograms of the H^+ population for spacecraft 1, 3 and 4, the magnetic field magnitude for all 4 spacecraft and the H^+ bulk speed for spacecraft 3 (the reference spacecraft of the Cluster configuration) as a function of time. There is no CIS data from spacecraft 2 due to the failure of the main power supply of CIS on this spacecraft. During the time period of interest, the spacecraft were transmitting data in burst mode, which provides ion distributions with the highest time resolution of CODIF, i.e. for every spin. CODIF was operated with its high geometric factor side (HS) on spacecraft 1 and 3 and with its low geometric factor side (LS) on spacecraft 4. The H^+ bulk speed is taken from HIA on the reference spacecraft. Only during the time period of 05:35–05:40 UT were all four spacecraft continuously and simultaneously in the solar wind. This can be seen from the narrow maximum of the proton flux below 1 keV, the low and steady magnetic field value and the solar wind speed of 410 km/s. During the first 5 min of the time interval, the spacecraft approached the bow shock several times, indicated by increases in the magnetic field, decreases in the bulk speed and a widening of the H^+ energy distributions. Each of the bow shock encounters is also supported by simultaneous magnetic field rotations (not shown here). At 05:41 UT, all four spacecraft cross the bow shock in the sequence spacecraft 4, spacecraft 1, spacecraft 3 and finally spacecraft 2. At 05:47 UT, spacecraft 1, 3 and 2 exit again from the magnetosheath in the reverse sequence and encounter the bow shock an additional three times until 06:00 UT in the same sequence, whereas spacecraft 4 remains downstream of the bow shock for the rest of this time period. It should be noted that an overshoot of the magnetic field strength over the average downstream value is observed on spacecraft 1, 2 and 4 during the first encounter with the bow shock, but not on spacecraft 3. Generally, there is no sign of upstream energetic particle populations during this time period, except perhaps a small contribution up to a few keV right in front of the bow shock. The general sequence of bow shock crossings for the Cluster spacecraft suggests that the relative speed between the spacecraft and the shock was relatively low during the entire time and that the spacecraft never entered deeply into the magnetosheath.

Figure 2 shows a schematic 3D representation of the local bow shock geometry and the configuration of the Cluster spacecraft during the time interval of interest. They were at $X = 8.2\ R_E$, $Y = 10.25\ R_E$ and $Z = 8.75\ R_E$ (GSE), i.e. at a distance of 15.75 R_E at the dusk flank and over the northern hemisphere. The interplanetary magnetic field (IMF) pointed earthward at 150° in azimuth and −20° in elevation. A minimum variance analysis of the magnetic field at the bow shock crossing at 05:41 UT returns an angle of Θ_{Bn} −70° between the IMF $\boldsymbol{B}$ and the shock normal $\boldsymbol{n}$. During this time, the bow shock is a very good example for a quasi-perpendicular shock. Under these conditions, a reflected distribution of gyrating ions is expected at the shock, and a reflected beam into the upstream direction may also develop. Possible trajectories of specularly reflected ions of the incoming solar wind in the pertinent IMF are also shown in Fig. 2. We will use this time interval with the availability of high time resolution data to study the spatial structure of the ion reflection in the shock region and the evolution of the ion distribution, from the upstream region into the shock ramp. Due to the almost erratic motion of the shock across the spacecraft, and its reversal several times in direction, this time period is not suitable to follow the thermalization of the ions downstream

into the magnetosheath.

3 Observations of reflected ion populations at the shock

As CODIF provides the full 3D velocity distribution of ions for every spacecraft spin, i.e. every 4 s, the evolution of the ion distribution from the upstream region into the shock can be studied at high time resolution and compared between the different Cluster spacecraft. Figure 3 shows a series of 4π views of angular distributions of the differential H^+ flux at 6 different energies for spacecraft 1, 3 and 4. Figure 3a shows the distributions upstream of the shock at 05:39 UT, Fig. 3b at the edge of the shock ramp at 5:41 UT, and Fig. 3c just 3 spacecraft spin periods (12 s) further into the shock ramp at 05:41:12 UT. All times are given for the reference spacecraft spacecraft 3. The times for spacecraft 1 and 4 have been chosen such that all views are shown exactly at the ramp edge in Fig. 3b for all 3 spacecraft, as obtained from magnetic field observations. The time separation between the spacecraft has been kept the same for all three figures. The time interval in the ramp (Fig. 3c) has been chosen so that the views from spacecraft 1 and 4 are simultaneous with those at the ramp edge (Fig. 3b) from spacecraft 3 and 1, respectively.

Directional distributions from 0.3 to 6 keV are shown in a globe representation. The individual views are oriented such that sector 0 (out of 16 from the operational mode in use) of the CODIF sectoring scheme with the spacecraft spin is at the left edge of each view. This brings the solar wind flow (coming from GSE-X) two sectors left of the center. To see the views of the low sensitivity side from spacecraft 4 in the same orientation, these views have been rotated by 180°. This compensates for instrument viewing in the opposite direction. Flows seen at the lower edge of the globes come at 90° from below and those at the upper edge come from above. Therefore, the intense flux in the center of the view, next to the star representing the magnetic field in the panels from 0.3 to 2.0 keV, represents the solar wind. The white star indicates the magnetic field pointing out of the plane of the figure. The solar wind is seen over such a large energy range, due to the high sensitivity of CODIF on its high geometric factor side. In fact, the solar wind saturates the sensor. Also found in Fig. 3a is a flux of a much lower intensity generally in the opposite direction of the solar wind and near a 180° pitch angle at energies from 0.8 to 6 keV (The white cross indicates the magnetic field pointing into plane of the figure). These ions stream away from the bow shock generally along the magnetic field lines, although the distribution is not exactly centered on the magnetic field direction, indicating a visible gyrophase bunching. The beam distribution is only faintly visible on spacecraft 4 because CODIF is operated on its low geometric side and thus the count rate is lower by almost two orders of magnitude.

In Figs. 3b and 3c, the solar wind and the beam distribution in the opposite direction are also visible. However, high particle fluxes are found near a 90° pitch angle over the same energy range as the beam as well. In fact, the distribution is

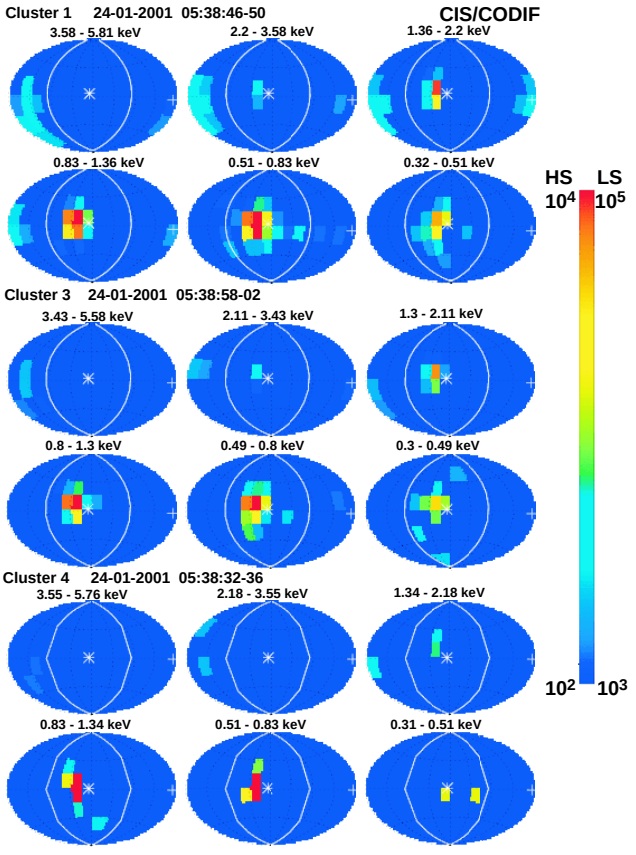

Fig. 3a. 4π angular distributions of the H^+ fluxes from CODIF in color-coded representation for 6 energies from spacecraft 1 (top), spacecraft 3 (center), and spacecraft 4 (bottom) ≈ 1 min before bow shock entry. Shown is the instrument view of the incoming particle flux. The white star indicates the magnetic field pointing out of the figure and the cross indicates the magnetic field pointing into the figure. The white line indicates a 90° pitch angle. The scaling of the color bar (in differential flux) is higher by a factor of 10 for the low sensitivity (LS) mode of CODIF on spacecraft 4, because in high sensitivity (HS) mode, the sensor saturates at the lower maximum flux levels chosen for spacecraft 1 and 3.

spread over a wide pitch angle range in the lower left portion of the angular map, with the particles flowing in from below at the lowest energies. With increasing energy, the velocity vector of the maximum flux of this reflected distribution turns more and more to 0° in elevation. This behaviour is similar on spacecraft 1, 3 and 4. Due to its higher flux than that of the beam, this component is clearly visible on spacecraft 4 in spite of the lower geometric factor.

When comparing Figs. 3b and 3c to each other, they appear to be very similar at first glance. However, upon closer inspection, they reveal subtle differences between the two time intervals on the same spacecraft, but not between the individual spacecraft during the same interval. The data were taken only 12 s (3 spin periods) apart. During these 12 s the peak of the reflected distribution moved towards lower pitch angles in the same hemisphere of the solar wind, when the spacecraft are somewhat further into the shock ramp

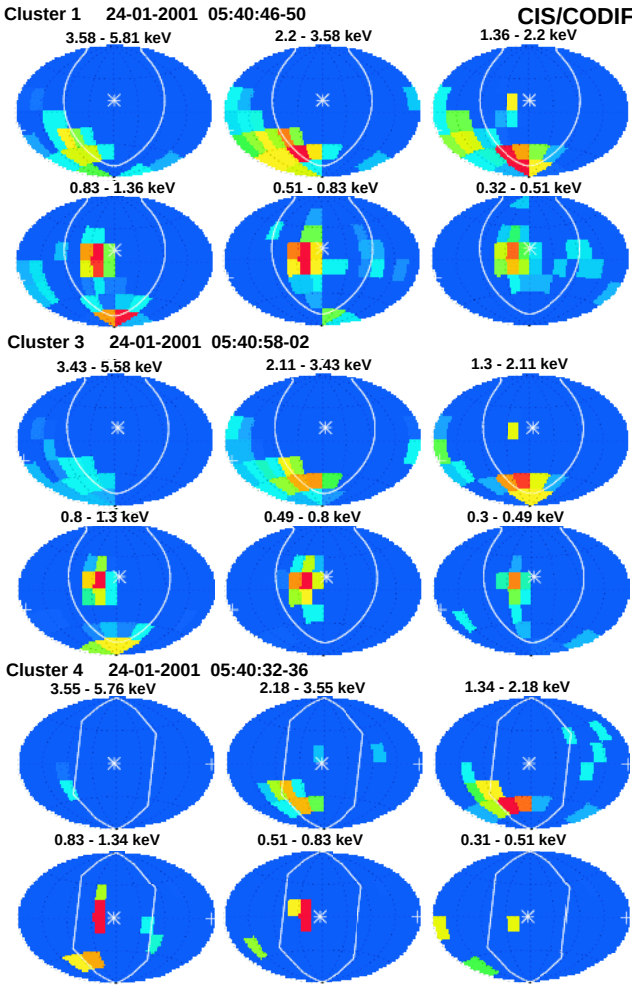

Fig. 3b. Similar representation as Fig. 3a exactly at the edge of the shock ramp. The fact that no counts are seen in the pole pixels at the bottom for spacecraft 4 is due to the fact that the corresponding angle range is blind at both poles on the low sensitivity side in order to prevent spillover from the high sensitivity side of the sensor.

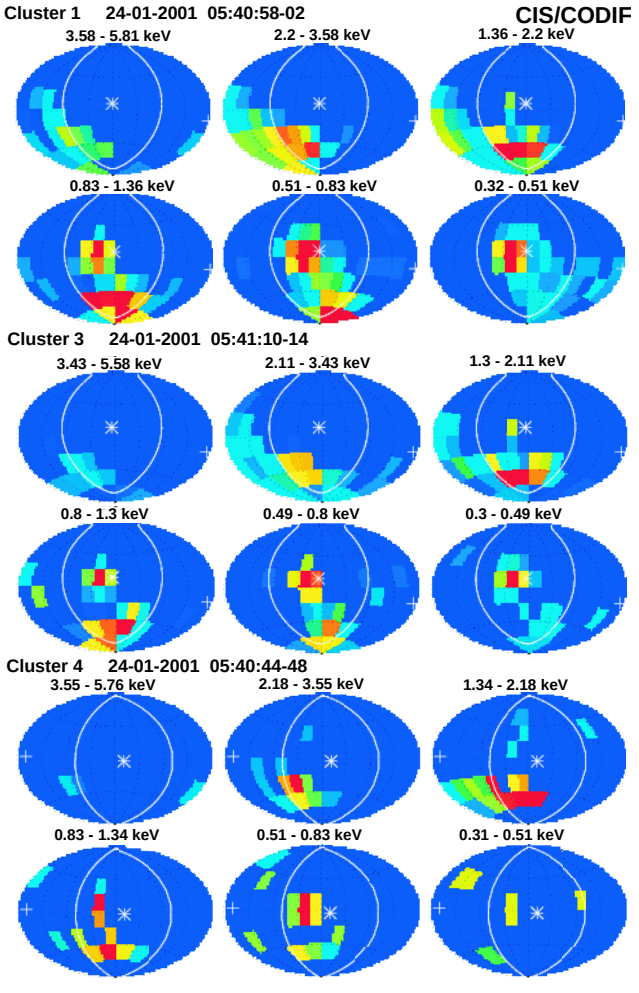

Fig. 3c. Similar representation as Fig. 3b, 3 spacecraft spin periods later into the shock ramp.

(Fig. 3c). The peak is found almost exactly at a 90° pitch angle, when the spacecraft are exactly at the edge of the shock ramp (Fig. 3b). This shift of the peak is consistent on all three spacecraft, i.e. they observe exactly the same reflected ion topology, but are time shifted according to their individual arrival times at the shock. Therefore, this observation is consistent with a spatial structure that is coherent over the distance between the three spacecraft.

Over the separation distance of the Cluster spacecraft the reflected ion population appears homogeneous. In addition, the morphology of the shock remains unchanged during the entire observation time period as the shock sweeps repeatedly across the spacecraft. A persistent observation during this time interval is a reflected ion population that appears in a wide range of pitch angles and is partially swept downstream with the magnetic field and partially escapes into the upstream region. The most prominent portion of the reflected particles near the 90° pitch angle is convected downstream with the IMF and is only visible immediately upstream of the shock. It has disappeared on the view that is taken −1 min before the shock crossing (Fig. 3a). However, a reflected ion beam seems to emerge from the very wide pitch angle distribution of the reflected population that is seen close to the shock at the extreme end of the low pitch angles in the direction opposite to the solar wind. These particles have a high enough velocity component parallel to $\boldsymbol{B}$ in the upstream direction so that they can escape against the downstream transport with the magnetic field.

Referring to Fig. 2, the shock geometry and the solar wind flow at the northern evening flank conspire so that ions, which are specularly reflected in the shock potential, emerge from the potential generally in the upward (Z) direction and slightly into the Y direction. This direction is consistent with the observed particles seen in the lowest energy panels (0.3–0.8 keV) in Fig. 3c. The peak of these reflected ions is seen to the lower right of the center in these panels. With respect to the magnetic field, their nominal direction is close to the 90° pitch-angle and slightly into the downstream direction. Thus, all reflected ions should be swept downstream.

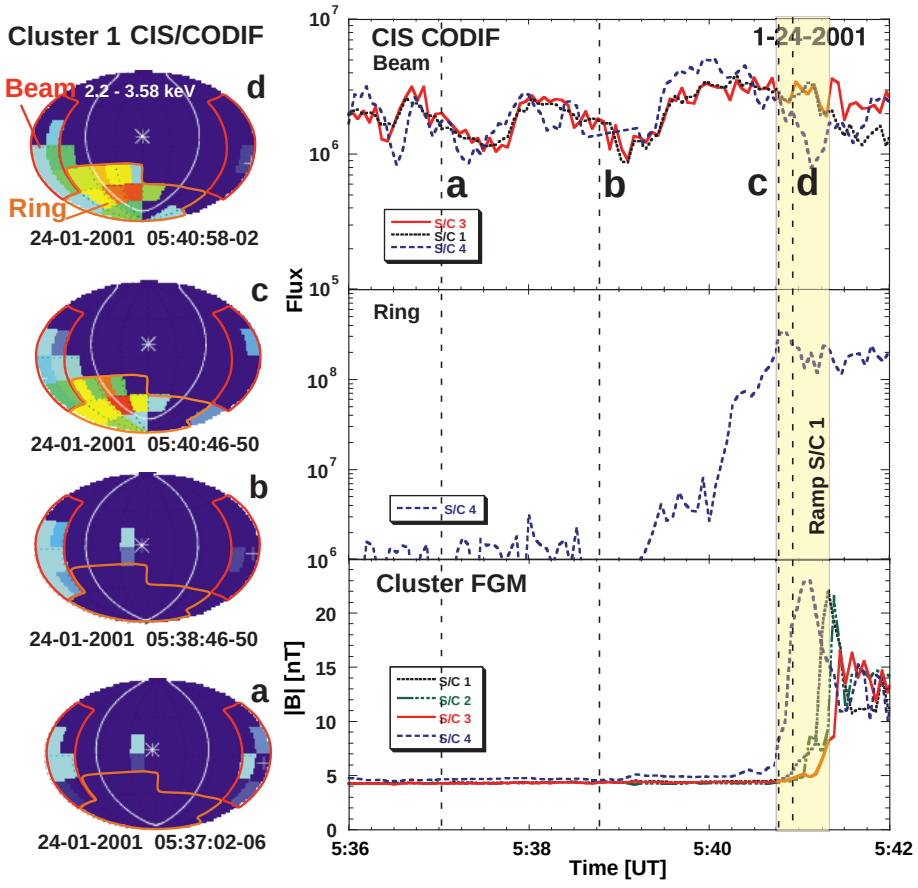

Fig. 4. Left column: Angular distributions as seen on spacecraft 1 in the shock ramp **(d)**, at the ramp edge **(c)**, and upstream of the shock **(b), (a)**. The angular regions of the beam (red) and ring (orange) are indicated. Right column: Integrated H^+ flux in the phase space portions that represent the beam from spacecraft 1, 3 and 4 (upper panel), reflected ring from spacecraft 4 (center panel), and magnetic field strength from all four spacecraft (lower panel). They are shown from approximately 5 min before the bow shock encounter through the shock ramp.

However, from their origin in the shock ramp these ions appear to be spread over a wide pitch angle range, rather than sharply peaked at the specific pitch angle of specular reflection. However, the fluxes vary substantially over the angular range, and only with a very sensitive instrument can the entire distribution be observed. The full distribution thus appears wider than the typical ring and beam distributions previously reported for the quasi-perpendicular bow shock. Apparently, both the ring distribution that is ultimately swept downstream and the beam that escapes upstream are intimately linked and emerge from the same reflection process. There must be additional scattering processes at work that widen the relatively narrow distribution, as may have been expected from specular reflection in the orderly shock potential of a quasi-perpendicular shock.

In order to illustrate that the ion beam indeed emerges from the combined ring distribution at the shock and to study the spatial and temporal behaviour of these distributions, we have subdivided angular space into a beam and a ring domain. Figure 4 shows the angular distributions from spacecraft 1 in the peak energy region of the ring and beam (2.2–3.6 keV) for four 4 intervals on the left. In the same figure, the temporal variation of the beam and ring population fluxes, along with the magnetic field magnitude for all four spacecraft are shown on the right. The beam portion is indicated by a red line, and the ring portion is indicated by an orange line in the four angular distributions. We have integrated the ion fluxes separately over these two solid angle domains and the full energy range of the beam and ring for spacecraft 1, 3 and 4. The resulting total fluxes for the beam have been compiled as a function of time in the upper right panel. The center right panel shows the total flux of the ring distribution as obtained on spacecraft 4. We do not show spacecraft 1 and 3 here, because the full ring fluxes saturate CODIF in its high sensitivity mode by about one order of magnitude, while the sensor is not saturated in its low sensitivity mode on spacecraft 4. The shaded vertical band indicates the passage of the shock ramp by spacecraft 1, and the magnetic field in the lower right panel shows when each spacecraft reaches the shock. The four time intervals of our angular distributions (a, b, c, and d) are indicated by vertical lines. Panel (a) has been taken almost two minutes further upstream than the view of the beam distribution in Fig. 3a. The other three panels (b, c and d) contain the same time

intervals as shown already in Fig. 3.

The observations presented in Fig. 4 demonstrate quite clearly the value of two substantially different geometric factors in CODIF. While the high sensitivity side of CODIF is saturated by the ring distribution which represents a large fraction of the solar wind flux, the low sensitivity side of CODIF is starved for counts in the beam distribution for the one spin time resolution observations discussed here. With a much higher count rate, the high sensitivity side of CODIF shows remarkable structure and time variation in the beam. For example, in view (a), i.e. substantially further upstream of the shock, the field-aligned beam is more gyrotropic than about two minutes later. Closer to the shock, the beam distribution apparently still has a memory of the original gyrophase, with which it was injected at the shock. With increasing distance this memory subsides because ions with different pitch angle and gyrophase start to mix. In addition, the beam flux varies on the time scale of less than one minute.

From downstream of the shock through the shock ramp the flux of the ring distribution (center right panel in Fig. 4) remains on a high level and falls off quickly by more than two orders of magnitude with distance from the shock. The ramp location as indicated in the figure is for spacecraft 1 in accordance with the angular distributions. Two minutes before the shock crossing, the flux in the ring domain is down to a very low value. The remaining fluxes seen further upstream are on the level of one or a few counts and thus, at the detection threshold for spacecraft 4.

The total flux in the beam distribution is about one order of magnitude lower than that in the ring distribution in the shock ramp, but the flux remains approximately constant (within a factor of three) with distance from the shock. The beam indeed appears to originate in the combined reflected ion distribution in the shock ramp. It emerges from the edge of this wide pitch angle distribution and then escapes more or less along the field lines under flux conservation. Therefore, the flux in the beam must depend on the angular width of the reflected distribution and on the pitch angle that is achieved after ideal specular reflection in the shock potential. These factors have to be taken into account in addition to the overall reflection efficiency for solar wind ions.

The beam fluxes on all three spacecraft (spacecraft 1, 3 and 4) track each other almost perfectly. As already discussed above, CODIF on spacecraft 4 has much poorer counting statistics, so that fluctuations around the much smoother spacecraft 1 and 3 observations are found. However, the spacecraft appear to pass a distinct spatial/temporal pattern in the beam distribution, as the fluxes vary distinctly and exactly simultaneously on all three spacecraft, with two flux minima at 05:37:30 UT and at 05:39:05 UT. The temporal variation in the beam fluxes appears to be distinctly different from that of the general shock motion, as indicated by the sequence of shock arrival in the magnetic field observations. The exact simultaneous occurence on all three spacecraft apparently reflects an intrinsic temporal variation of the beam fluxes as seen by at least three of the Cluster spacecraft. The observed pattern is, therefore, coherent over the spacecraft separation distance, i.e. 440 km (between spacecraft 3 and 4) to 750 km (between spacecraft 1 and 3), which is of the order of the ion gyro radius of solar wind protons. The unique combination of the high time resolution and the multi-spacecraft observations of Cluster make it possible to unambiguously separate the shock motion and this intrinsic variation of the beam.

4 Discussion, conclusions and outlook

We have observed the ion reflection processes at a quasi-perpendicular bow shock during a period when the shock repeatedly moved across the Cluster formation. The spacecraft remained close to the shock for an extended time, and the shock morphology apparently stayed the same. Generally, also the same particle distributions were observed throughout, although not discussed here in detail. The individual spacecraft passed through the shock structure and the reflected ion distributions in a consistent sequence, while the shock was moving across. Phase shifted by about 10 s between spacecraft 4 and 1, and by about 12 s between spacecraft 1 and 3; all three spacecraft encountered almost identical angular and energy distributions in the sequence spacecraft 4, 1 and 3 during the first shock transition. This indicates that a stable pattern of reflected ions is established at the bow shock that is coherent over the spacecraft separation distance and generally does not change substantially during the repeated shock crossings.

A detailed study of the velocity distribution of the reflected ions during this shock crossing has shown that the ring and beam distributions are intimately connected. The beam distribution that escapes from the shock along the magnetic field lines emerges from the low pitch angle wing of the reflected ring distribution in the shock ramp under flux conservation. When taken in the shock ramp the total flux of the ring distribution as observed on spacecraft 4 varies from 1.1 to $3.3 \cdot 10^8\,\mathrm{cm^{-2}\,s^{-1}}$ with an average of $1.9 \cdot 10^8\,\mathrm{cm^{-2}\,s^{-1}}$. The total flux of the beam is, on average, $2.3 \cdot 10^6\,\mathrm{cm^{-2}\,s^{-1}}$ with a minimum of $8.7 \cdot 10^5\,\mathrm{cm^{-2}\,s^{-1}}$ and a maximum of $3.9 \cdot 10^6\,\mathrm{cm^{-2}\,s^{-1}}$. With a solar wind flux of $9.5 \cdot 10^8\,\mathrm{cm^{-2}\,s^{-1}}$, as obtained with CIS HIA, this amounts to a fraction of the solar wind that is reflected in the ring distribution of 12–35%, or on average, 20.4%. In the field-aligned beam, about $0.25 \pm 0.15\%$ of the solar wind is found. Thus, the flux of the beam is only of the order of 1% of that found in the reflected ring distribution. The observed percentages of the solar wind for the ring and beam distributions agree with values given previously by Sckopke et al. (1990) and Thomsen (1985), respectively.

These results appear generally more consistent with the idea of the ion beam leaking out of a heated distribution downstream of the shock (Eichler, 1979; Thomsen et al., 1983) than a separate direct reflection of these beam ions. However, this would leave a puzzling observation that generally, the thermal distribution in the magnetosheath is not hot enough to account for the observed ion beams. The fact

that the beam, as observed upstream of the shock, has the same total flux as the respective pitch angle region of the reflected ring, suggests a different interpretation. The beam is, in fact, part of the ring distribution itself and is produced by effective pitch angle scattering during or immediately after the reflection, i.e. long before the ring is thermalized in the downstream region. Such a mechanism has recently been suggested in the form of cross-field diffusion at quasi-perpendicular shocks (e.g. Giacalone et al., 1994; Scholer et al., 2000). Simulations of the quasi-perpendicular shock indeed show that a very effective scattering by Alfvén waves is possible immediately downstream of the ramp (Scholer et al., 2000). Such a mechanism is also consistent with the observed fractions in the reflected distributions. Only a small fraction, typically $\approx 1\%$, of the ring distribution escapes into the upstream region. Future studies of reflected ion distributions as a function of parameters that control the shock, such as fast Mach number, Θ_{BN}, and Θ_{BV} (the angle with respect to the solar wind flow), will provide further insight into this important injection problem at quasi-perpendicular shocks.

In general, the flux of the reflected beam is conserved with distance from the shock. However, there is also an apparent intrinsic temporal variation in the fluxes of the field-aligned beam distribution that is seen simultaneously on three spacecraft and thus, must reflect a variation in the shock conditions. This result leaves the following question: what is the possible reason for the variation of the beam density across different magnetic flux tubes. There are several potential contributors to such a density variation in the beam; the overall reflection efficiency at the shock, the width of the reflected distribution in pitch angle, i.e. the scattering efficiency, and the nominal pitch angle after specular reflection in relation to Θ_{BN}. While we can only speculate about the first two parameters, since none of the Cluster spacecraft is actually in the shock ramp during this observation to assess these possibilities, we may test the possibility of a change in nominal pitch angle. In fact, the IMF shows moderate excursions in the elevation angle, occuring simultaneously on all spacecraft, when the variations in the beam flux are observed. Since the solar wind ions are reflected into the upward direction by the shock potential, more negative elevation angles would lead to a smaller pitch angle of the reflected ions, which should increase the beam flux. In our case, the variations in magnetic field elevation do not seem to correlate with the flux variations in the beam. However, the variations in IMF angle could also modify the shock reflection and scattering. At this point, this leaves us with speculative possibilities, and the explanation of this observation must await more detailed studies of reflected ion populations at the quasi-perpendicular shock under a variety of different conditions.

The results presented in this paper have clearly demonstrated how valuable the Cluster formation is for the study of complex spatial and time variable structures at the magnetospheric boundaries. Without the multiple spacecraft configuration, it would have been impossible to separate unambiguously the intrinsic temporal pattern in the ion beam flux from the repeatedly reversing motion of the bow shock across the spacecraft. Since both the quasi-perpendicular and the quasi-parallel bow shock regions and their complex particle distributions are inherently variable in space and time, Cluster and its instrumentation will reveal a number of new phenomena and will probe deeply into the related physical processes.

Acknowledgements. We wish to thank the many unnamed individuals at the CESR Toulouse, at the University of New Hampshire, at the Max-Planck-Institut für extraterrestrische Physik, Garching, and für Aeronomie, Lindau, at the University of California, Berkeley, at the University of Washington, at IFSI, Frascati, at the Lockheed Martin Advanced Technology Lab, Palo Alto, at the Institute for Space Physics, Kiruna, and at the Universität Bern for their dedicated work towards the successful completion of the Cluster CIS experiment for Cluster I and II. This work was supported by CNES, by NASA under Contract NAS5-30613 and Grant NAG5-10131, by ESA under Contract 1501073–2400, by Deutsches Zentrum für Luft- und Raumfahrt under Contracts 50 OC 8906, 50 OC 89030 and 50 OC 0102, by the Swiss National Science Foundation, and the University of the Kanton Bern. The authors thank M. A. Lee for valuable discussions during the preparation of this paper.

The Editor in Chief thanks S. Bale and another referee for their help in evaluating this paper.

References

Asbridge, J. R., Bame, S. J., and Strong, I. B.: Outward flow of protons from the Earth's bow shock, J. Geophys. Res., 73, 5777, 1968.

Axford, W. I., Leer, E., and Skadron, G.: The acceleration of cosmic rays by shock waves, Proc. 15th Int. Conf. Cosmic Rays, 11, 132, 1977.

Balogh, A., Dunlop, M. W., Cowley, S. W. H., Southwood, D. J., Thomlinson, J. G., Glassmeier, K. H., Musmann, G., Lühr, H., Buchert, S., Acuña, M. H., Fairfield, D. H., Slavin, J. A., Riedler, W., Schwingenschuh, K., Kivelson, M. G., and the Cluster Magnetometer Team: The Cluster Magnetic Field Investigation, Space Sci. Rev., 79, 65, 1997.

Burgess, D.: Cyclic behaviour at quasi-parallel collisionless shocks, Geophys. Res. Lett., 16, 345, 1989.

Eichler, D.: Particle acceleration in collisionless shocks: Regulated injection and high efficiency, Astrophys. J., 229, 419, 1979.

Formisano, V.: Collisionless shock waves in space and in astrophysics, in: Proc. ESA Workshop on Future Missions in Solar, Heliospheric & Space Plasma Physics, ESA-SP, 235, 83, 1985.

Giacalone, J., Jokipii, J. R., and Kota, J.: Ion injection and acceleration at quasi-perpendicular shocks, J. Geophys. Res., 99, 19 351, 1994.

Gosling, J. T., Asbridge, J. R., Bame, J., Paschmann, G., and Sckopke, N.: Observation of two distinct populations of bow shock ions in the upstream solar wind, Geophys. Res. Lett., 5, 957, 1978.

Gosling, J. T. and Robson, A. E.: Ion reflection, gyration, and dissipation at supercritical shocks, in: Collisionless Shocks in the Heliosphere: Reviews of Current Research, (Eds) Tsurutani, B. T. and Stone, R. G., Geophys. Monograph, 35, 141, 1985.

Ipavich, F. M., Gloeckler, G., Hamilton, D. C., Kistler, L. M., and Gosling, J. T.: Protons and alpha particles in field-aligned beams upstream of the bow shock, J. Geophys. Res., 86, 4337, 1981.

Lee, M. A., Shapiro, V. D., and Sagdeev, R. Z.: Pickup ion energization by shock surfing, J. Geophys. Res., 101, 4777, 1996.

Lin, R. P., Meng, C. I., and Anderson, K. A.: 30 to 100 keV protons upstream from the Earth's bow shock, J. Geophys. Res., 79, 489, 1974.

Möbius, E.: Studies with Cluster upstream and downstream of the bow shock – An experimenter's perspective, ESA-SP, 371, 127, 1995.

Möbius, E., Kistler, L. M., Popecki, M., Crocker, K., Granoff, M., Jiang, Y., Sartori, E., Ye, V. Rème, H., Sauvaud, J. A., Cros, A., Aoustin, C., Camus, T., Médale, J. L., Rouzaud, J., Carlson, C. W., McFadden, J. P., Curtis, D. W., Heetderks, H., Croyle, J., Ingraham, C., Shelley, E. G., Klumpar, D., Hertzberg, E., Klecker, B., Ertl, M., Eberl, F., Kästle, H., Künneth, E., Laeverenz, P., Seidenschwang, E., Parks, G. K., McCarthy, M., Korth, A., Gräwe, B., Balsiger, H., Schwab, U., and Steinacher, M.: The 3-D plasma distribution function analyzers with time-of-flight mass discrimination for Cluster, FAST and Equator-S, in: Measurement Techniques in Space Plasmas, (Eds) Pfaff, R., Borowski, J., and Young, D., Geophys. Monograph, 102, 243, 1998.

Paschmann, G., Sckopke, N., Asbridge, J. R., Bame S. J., and Gosling, J. T.: Energization of solar wind ions by reflection from the Earth's bow shock, J. Geophys. Res., 85, 4689, 1980.

Paschmann, G. and Sckopke, N.: Ion reflection and heating at the Earth's bow shock, in: Topics in Plasma-, Astro- and Space Physics, (Eds) Haerendel, G. and Battrick, B., p. 139, Max-Planck-Institut für Physik und Astrophysik, Garching, Germany, 1983.

Quest, K. B.: Theory and simulation of collisionless parallel shocks, J. Geophys. Res., 93, 9649, 1988.

Rème, H., Bosqued, J. M., Sauvaud, J. A., Cros, A., Dandouras, J., Aoustin, C., Martz, Ch., Médale, J. L., Rouzaud, J., Möbius, E., Crocker, K., Granoff, M., Kistler, L. M., Hovestadt, D., Klecker, B., Paschmann, G., Ertl, M., Künneth, E., Carlson, C. W., Curtis, D. W., Lin, R. P., McFadden, J. P., Croyle, J., Formisano, V., DiLellis, M., Bruno, R., Bavassano-Cattaneo, M. B., Baldetti, B., Chionchio, G., Shelley, E. G., Ghielmetti, A. G., Lennartson, W., Korth, A., Rosenbauer, H., Szemerey, I., Lundin, R., Olson, S., Parks, G. K., McCarthy, M., and Balsiger, H.: The CLUSTER Ion Spectrometry Experiment, Space Sci. Rev., 79, 303, 1997.

Rème, H., Aoustin, J. M., Dandouras, I., Lavraud, B., Sauvaud, J. A., Barthe, A., Bouyssou, J., Camus, Th., Coeur-Joly, O., Cros, A., Cuvilo, J., Ducay, F., Garbarowitz, Y., Medale, J. L., Penou, E., Perrier, H., Romefort, D., Rouzaud, J., Alcayde, D., Jacquey, C., Mazelle, C., d'Uston, C., Möbius, E., Kistler, L. M., Crocker, K., Granoff, M., Moukis, C., Popecki, M., Vosbury, M., Klecker, B., Hovestadt, D., Kucharek, H., Künneth, E., Paschmann, G., Scholer, M., Sckopke, N., Carlson, C. W., Curtis, D. W., Ingraham, C., Lin, R. P., McFadden, J. P., Parks, G. K., Phan, T., Formisano, V., Amata, E., Bavassano-Cattaneo, M. B., Baldetti, P., Bruno, R., Chioncho, G., DiLellis, A., Marcucci, M. F., Korth, A., Daly, P. W., Graeve, B., Rosenbauer, H., Vasyliunas, V., McCarthy, M., Wilber, M., Eliasson, L., Lundin, R., Olsen, S., Shelley, E. G., Fuselier, S., Ghielmetti, A. G., Lennartsson, W., Escoubet, C. P., Balsiger, H., Friedel, R., Cao, J. B., Kovrazhkin, R. A., Papamastorakis, I., Pellat, R., Scudder, J., and Sonnerup, B.: First identical multispacecraft ion measurements in and near the Earth's magnetosphere with the Cluster Ion Spectrometry (CIS) experiment, Ann. Geophysicae, this issue (2001).

Scholer, M., Gloeckler, G., Ipavich, F. M., Hovestadt, D., and Klecker, B.: Pitch-angle distributions of energetic protons near the Earth's bow shock, Geophys. Res. Lett., 6, 707, 1979.

Scholer, M. and Terasawa, T.: Ion reflection and dissipation at quasi-parallel collisionless shocks, Geophys. Res. Lett., 17, 119, 1990.

Scholer, M., Kucharek, H., and Giacalone, J.: Cross-field diffusion of charged particles and the problem of ion injection and acceleration at quasi-perpendicular shocks, J. Geophys. Res., 105, 18 285, 2000.

Sckopke, N., Paschmann, G., Brinca, A. L., Carlson, C. W., and Lühr, H.: Ion thermalization in quasi-perpendicular shocks involving reflected ions, J. Geophys. Res., 95, 6337, 1990.

Sonnerup, B. U. Ö.: Acceleration of particles reflected at a shock front, J. Geophys. Res., 74, 1301, 1969.

Thomsen, M. F., Gosling, J. T., Bame, S. J., Feldman, W. C., Paschmann, G., and Sckopke, N.: Fieled-aligned ion beams upstream of the earth's bow shock: Evidence for a magnetosheath source, Geophys. Res. Lett., 10, 1207, 1983.

Thomsen, M. F.: Upstream suprathermal ions, in: Collisionless Shocks in the Heliosphere: Reviews of Current Research, (Eds) Tsurutani, B. T. and Stone, R. G., Geophys. Monograph, 35, 235, 1985.

West, H. I. and Buck, R. M.: Observations of >100 keV protons in the Earth's magnetosheath, J. Geophys. Res., 81, 569, 1976.